

Journal of Hydraulic and Water Engineering (JHWE)

Iranian Hydraulic Association (IHA)

Journal homepage: https://jhwe.shahroodut.ac.ir

Assessment of Climate Change Impacts on the Hydrological Behavior of the Sarbaz River Basin Using CMIP6 Climate Models

Amirhossein Shahrakizad*1

¹Department of Civil Engineering and Water Resources Management, University of Sistan and Baluchistan, Zahedan, Iran.

Abstract Article Info Article history: This study introduces a framework for assessing climate change and flow Received 29 May 2025 conditions by integrating the latest climate simulations from the CMIP6 project Received in revised form 25 June (HadGEM3-GC31-LL model) with the Soil and Water Assessment Tool (SWAT) Accepted 08 July 2025 and evaluating the influence of different climate model resolutions. A total of 66 Published online 10 July 2025 hydrological and environmental flow indicators from the Indicators of Hydrologic Alteration (IHA) were calculated to assess future extreme flows in the Sarbaz River Basin, located in Sistan Province, which is particularly vulnerable to 10.22044/JHWE.2025.16321.1068 flooding. Results indicate that by the 2030–2050 period, compared to the baseline period of 1990-2019, annual precipitation, streamflow, and maximum and Kevwords minimum temperatures are projected to increase by 6.9%, 9.9%, 0.8°C, and 0.9°C, Climate Change respectively. Monthly precipitation and streamflow are expected to rise, Sarbaz River Basin SWAT Model especially during the monsoon season (June-September) and early wet periods CMIP6 Models Hydrologic (December). The magnitude of minimum 1-, 3-, 7-, 30-, and 90-day flows is Indicators (IHA) projected to increase by 7.2% to 8.2%, while peak flows could rise by 10.4% to 28.4%. Finally, significant differences were observed between high- and lowresolution climate models, with high-resolution models predicting an 11.8% increase in average monthly flows during November-January, compared to just 3.2% in low-resolution models.

1. Introduction

The increasing frequency and severity of extreme climate events, such as droughts and floods, are largely linked to climate change. causing serious social and economic impacts (Giorgi et al., 2018; Raikes et al., 2019). Scientific studies show that global warming, mainly caused by human-emitted greenhouse gases, poses a significant threat to the environment, ecosystems, and human societies. In recent decades, Asia has faced increased rainfall and higher temperatures due to global warming (Tan et al., 2021; Tong et al., 2019). These changes significantly affect hydrological systems, increasing water-related risks such as floods and droughts (François et al., 2019; Kundzewicz et al., 2014). Severe droughts can reduce

agricultural productivity and freshwater resources, leading to social and economic losses (Balti et al., 2020). To assess trends in hydro-climatic extremes in a specific region, long-term observational data are essential, as they provide the most reliable source for understanding the hydro-climatic system (Fu et al., 2010). Long-term observational data are crucial for analyzing hydro-climatic extremes, with hydrological models whether distributed (e.g., SWAT) or semidistributed (e.g., AWBM, IHACRES) essential tools for understanding these evaluating mitigation processes and strategies. These models are versatile, costeffective, and applicable across various scales. Additionally, outputs from Global

Climate Models (GCMs) are valuable for simulating climate-hydrology interactions (Ghorbani Fard, 2022; Shepherd et al., 1999; Singh and Woolhiser, 2002; Borah and Bera, 2004; Daniel, 2011; Fu et al., 2019; Betts et al., 2018). Vannière et al. used the highresolution HadGEM3A-GA3.0 model (~60 km) within CMIP5 to study the impacts of RCP8.5 on global freshwater flows, finding significant regional variations, with river flows in South and East Asia increasing up to twice the historic average (Vannière et al., 2019). The newer CMIP6 models, part of Phase 6 of the CMIP, feature advanced capabilities but still have coarse resolutions (100-200 km) (Eyring et al., 2016; Kim et al., 2020; Haarsma et al., 2016). Studies on Southeast Asia indicate spatially varied changes in river streamflow, with projections under the CORDEX-SEA framework suggesting drier conditions in southern regions and wetter conditions in the north by the end of the 21st century (Raghavan, 2013; Okwala et al., 2020; Supari et al., 2020). A study on Southeast Asia's hydroclimatic conditions (SEA-HOT) combined Regional Climate Models (RCMs) from the CORDEXframework **SEA** with the **SWAT** hydrological model to evaluate meteorological droughts under current and future climates. While RCMs provide highresolution climate data, they face limitations, such as the lack of two-way interactions with large-scale atmospheric patterns (Bowden et al., 2012; Harris et al., 2010). The SWAT model is widely used for hydrological simulations and watershed runoff analysis, supporting water resource management and environmental research (Arnold et al., 1998: Arnold et al., 2012a; Williams et al., 2008; Bieger et al., 2017). Today, SWAT is one of the most widely used hydrological models globally, applied to various water resource issues across different watershed sizes and 2019). environments (CARD, performance has been evaluated in four main ways: general assessments of flow and sediment, land management and erosion studies. region-specific analyses. and

applications of water management strategies. Overall reviews highlight SWAT's applications, performance, and future research directions (Gassman et al., 2007). Numerous thematic studies demonstrate simulating SWAT's effectiveness in streamflow and assessing climate change impacts (Krysanova and White, 2015; Gassman et al., 2014; Douglas-Mankin et al., 2010; Gassman and Wang, 2015; Tuppad et al., 2011). As SWAT's global use expands, synthesizing its findings helps developers and new users identify practical applications, model strengths, and key challenges in specific regions. Regional reviews have been conducted for the Upper Nile River Basin (van Griensven et al., 2012), Brazil (Bressiani et al., 2015), Southeast Asia (Tan et al., 2019a), and the Talar watershed, where the model was evaluated using both global and regional soil maps. Calibration with the SUFI-2 algorithm indicated that SOL AWC parameter was highly sensitive, and the regional soil map yielded more accurate results in certain sub-basins (Mohseni et al., 2023). Additionally, emerging applications include ecohydrological modeling (Krysanova and 2008), ecosystem Arnold, services (Francesconi et al., 2016), pesticide fate and transport (Wang et al., 2019), and daily-scale studies (Brighenti et al., 2019). Therefore, this study aims to introduce a novel framework for assessing the impacts of climate change on river flow in tropical regions by integrating the SWAT model indices, CMIP6 data, and IHA indicators. The main objectives of this research are: (1) to evaluate the capability of CMIP6 models at the basin scale; (2) to assess the performance of the SWAT model in longterm streamflow simulation; (3) to quantify hydrological variables for the periods 1990– 2019 and 2030-2050 under various CMIP6 GCM scenarios with both high and low spatial resolutions. The results provide a deeper understanding of how CMIP6 spatial resolution affects the accuracy of streamflow simulations. Moreover, this study presents a

comprehensive and up-to-date framework for evaluating future climatic conditions in Sistan and Baluchestan province and other tropical regions in developing and less developed countries, which can serve as a basis for climate adaptation strategies and environmental protection policies.

2. Materials and Methods2.1. Study Area

The Sarbaz watershed is the upstream basin of the Pishin Dam. It is one of the sub-basins of the rivers in Balochistan, located within the province and bounded by the coordinates 60°56′ to 61°35′ E and 26°5′ to 27°0′ N. To the east, it borders Pakistan; to the south, it is adjacent to Bahu Kalat and Dashtiari; to the west, it is limited by the Kajo watershed; and to the north, it is bounded by the Makran mountain range. This watershed, upstream of the Pishin hydrometric station, has an

average elevation of 932 meters above sea level. The basin covers 6,324 square kilometers and has an average slope of 16.8%.

The Sarbaz River is the only permanent river in Balochistan. The basin's northern regions predominantly influence the flow of the Sarbaz River. The river's base flow is very low, while its flood flow is significant even at low return periods. The river features both a large and a small riverbed. The river's flow regime corresponds to the precipitation pattern in summer and winter. The peak summer flows are primarily influenced by monsoon rainfall, whereas the peak winter flows are caused by precipitation from cold fronts originating from Siberia and the Mediterranean. Figure 1 illustrates geographical location of the Sarbaz watershed.

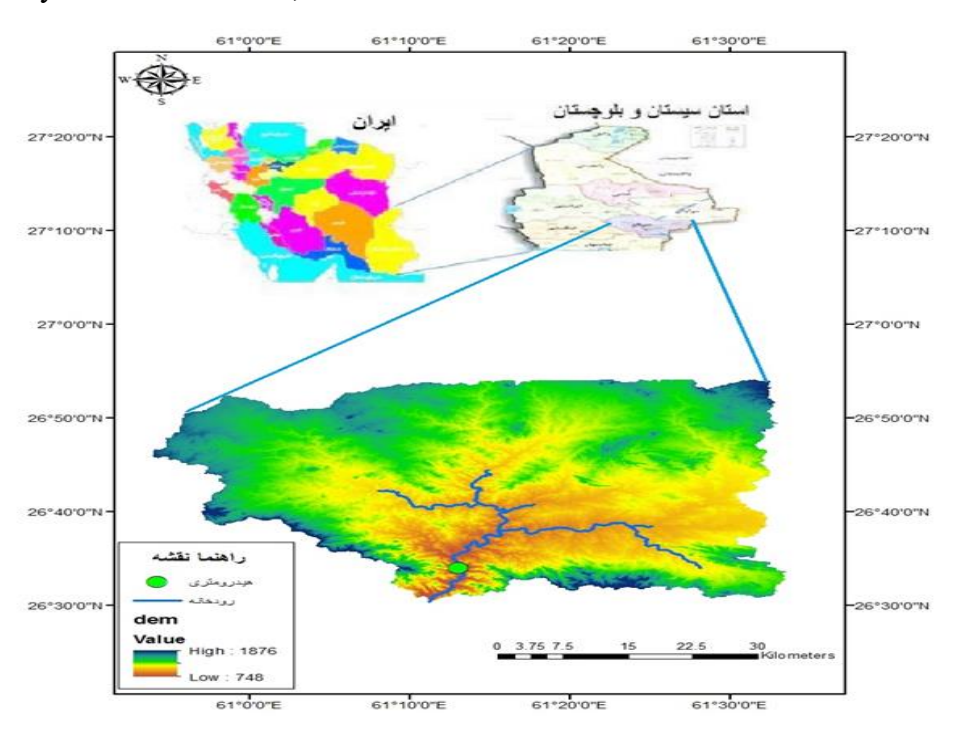


Figure 1. Study area

2.2. SWAT Model

The Soil and Water Assessment Tool (SWAT) is a semi-distributed, continuous-time hydrological model developed to assist water resource managers in evaluating the impacts of various land management practices on river

discharge and non-point source pollution (Arnold et al., 1998). Over the past few decades, SWAT has undergone numerous developments and enhancements (Gassman et al., 2007; Arnold et al., 2012). The model typically operates at a daily or monthly time

step and is designed for long-term continuous simulation. SWAT can be used for simulating long-term hydrology and climate patterns. While it performs well for average streamflow analysis, it requires high-resolution temporal input—at least daily—to adequately simulate extreme flood events. For robust climate studies that include both severe droughts and floods, long-term climatic data covering at least 30 years at daily resolution is recommended as input for SWAT simulations (Tan et al., 2020). Model calibration is essential for ensuring the reliability of SWAT outputs, and this is commonly achieved through the SWAT-CUP tool, which incorporates various optimization algorithms (Abbaspour et al., 2007; 2018). these, the Among SUFI-2 (Sequential Uncertainty Fitting Version 2) algorithm is widely used for calibrating SWAT at both daily and monthly time scales. Model performance is typically evaluated using statistical indices such as the coefficient of determination (R²) and the Nash-Sutcliffe Efficiency (NSE) (Nash et al., 1970). The values of R² range from 0 to 1, while NSE ranges from -1∞ to 1, with 1 indicating perfect model performance (Zhang et al., 2020).

2.3 CMIP6 Climate Models

Climate projections are recognized as a significant of uncertainty source in hydrological and hydroclimatic modeling studies focused on future conditions (Tan et al., 2014; Kundzewicz et al., 2018). These uncertainties arise from multiple factors, including future socio-economic development scenarios, greenhouse gas emissions, aerosol emissions. the sensitivity of General Circulation Models (GCMs) and regional (RCMs), downscaling climate models techniques, and bias correction methods. Minimizing these uncertainties is regarded as a critical future research priority (Kundzewicz et al., 2018). The CMIP3, CMIP5, and CMIP6

climate modeling frameworks have progressively enhanced our understanding of the Earth's future climate system (IPCC, 2013). In particular, CMIP6 GCMs have been widely used in conjunction with SWAT to evaluate the long-term impacts of climate change on river flows. The sixth phase of CMIP (Coupled Model Intercomparison Project), coordinated by LLNL (2019), serves as a key input to the IPCC Sixth Assessment Report (AR6). The latest high-resolution GCM outputs (<50 km) from the HighResMIP experiment significantly improve spatial resolution compared to the coarse outputs from CMIP5 models (Forsythe et al., 2019). These high-resolution simulations are comparable to those used in RCM-based studies (Musie et al., 2020; Tessema et al., 2020) and are expected to be increasingly applied in future SWAT-based studies. Given that climate change impact analysis is one of the primary applications of the SWAT model (Tan et al., 2019a; Gassman et al., 2014; CARD, 2019), this study adopts a selection of CMIP6 models based on their statistical performance during the historical (1990–2014) and future (2030–2050) periods. The climate data are sourced from the Earth System Grid Federation (ESGF) data platform. The SSP5-8.5 scenario drives simulations for the future period—a high-emission pathway within the new Shared Socioeconomic Pathways (SSPs) framework adopted by the IPCC for AR6. It is acknowledged that using only one climate scenario (SSP5-8.5)limits the comprehensiveness of the climate change impact assessment. Future studies incorporate additional scenarios such as SSP2-4.5 to provide a more balanced evaluation of different emission pathways and implications for water resources. Details of the selected GCMs, including model developers and horizontal resolution, are presented in Table 1.

Abbreviation	Resolution (Longitude ×Latitude)	Vertical Resolution (Layers)	Model Name	Modeling Organizations
HadGEM3-LM HadGEM3-MM HadGEM3-HM	$1.875^{\circ} \times 1.25^{\circ}$ $0.83^{\circ} \times 0.56^{\circ}$ $0.35^{\circ} \times 0.23^{\circ}$	85	HadGEM3- GC31	The UK Met Office Hadley Centre for Climate Change
CNRM CNRM-HR	$1.406^{\circ} \times 1.406^{\circ} \\ 0.5^{\circ} \times 0.5^{\circ}$	91	CNRM-CM6-1	French National Centre for Meteorological Research
EC-Earth	0.703° × 0.703 °	91	EC-Earth3P	27 institutes in Europe (Haarsma et al., 2020)
MRI-H MRI-S	$0.563^{\circ} \times 0.563^{\circ} \\ 0.188^{\circ} \times 0.188^{\circ}$	60	MRI-AGCM3-2	Meteorological Research Institute (Japan)
FGOALS-L	1.25° × 1 °	32	FGOALS-f3	Institute of Atmospheric Physics/Chinese Academy of Sciences
GFDL	0.625° × 0.5°	33	GFDL- CM4C192	Geophysical Fluid Dynamics Laboratory/ NOAA (U.S.)

Table 1. Summary of GCMs used in the CMIP6 experiments

The selection of climate models, particularly the HadGEM3-GC31-LL model and other HighResMIP models, was based on a combination of scientific performance criteria and practical considerations. The following key factors were used to guide the model selection process:

1-Spatial Resolution: HighResMIP models offer significantly higher spatial resolution than standard CMIP6 models, enabling a more accurate representation of regional climate features, especially in areas with complex topography or localized precipitation patterns. Performance 2-Model in Historical Simulations: Models were evaluated based on their ability to reproduce observed historical climate conditions, particularly temperature and precipitation trends over the study period. Models that showed better agreement with observational datasets (e.g., CRU, GPCC, and ERA5) were prioritized.

3-Availability of Required Variables: Only models that provide the necessary climatic variables (e.g., daily precipitation, maximum

and minimum temperatures, solar radiation) for both historical and future projection periods were considered.

4-Previous Use in Regional Studies: Preference was given to models that have been successfully applied in similar climatic regions, particularly in tropical and subtropical catchments in Southeast Asia and South Asia, where rainfall-runoff processes are susceptible to changes in precipitation patterns.

5-Data Accessibility: The availability of biascorrected and downscaled model outputs through reliable platforms, such as the Earth System Grid Federation (ESGF), was also considered to ensure consistency and reproducibility.

Based on these criteria, the HadGEM3-GC31-LL model from the HighResMIP ensemble was selected as the primary model for detailed analysis due to its superior performance in capturing seasonal rainfall variability and its high-resolution representation of hydrological processes.

Table 2	Results	of climate	model	evaluation

Model Name	Spatial Resolution	Historical Performance (Correlation with Observed Rainfall)	Extremes Representation	Data Availability	Regional Applicability
HadGEM3-GC31	High $(0.5^{\circ} \times 0.5^{\circ})$	Good (r = 0.82)	Very Good	Complete	High
CNRM-CM6-1	Medium $(1.4^{\circ} \times 1.4^{\circ})$	Moderate $(r = 0.65)$	Moderate	Complete	Moderate
EC-Earth3P	Medium $(0.7^{\circ} \times 0.7^{\circ})$	Moderate $(r = 0.68)$	Moderate	Complete	Moderate
MRI-AGCM3-2	High $(0.56^{\circ} \times 0.56^{\circ})$	Good (r = 0.78)	Good	Limited	High

2.4 IHA Indicators

The Indicators of Hydrologic Alteration (IHA) is a user-friendly tool developed by The Nature Conservancy to measure flow characteristics using 32 IHA indicators (Table 3) and 34 Environmental Flow Components (EFC) indicators (Table 4) [Richter et al., 1996]. For example, the IHA tool can calculate the magnitude and duration of annual minimum and maximum flows over specific periods such as 1-day, 3-day, 7-day, 30-day, and 90-day intervals. These indicators provide policymakers, water managers, hydrologists, and researchers with valuable information to

understand the impacts of human activities, including land use and anthropogenic climate change, on rivers and groundwater systems. Comparative analyses can be performed to describe and quantify changes in extreme hydrologic elements associated with climate change. The "zero flow days" indicator was excluded from this study due to its limited relevance in tropical regions. IHA version 7.1 was used to calculate extreme flows based on SWAT model outputs, with computations relying on daily flow data generated from the SWAT simulations.

Table 3. List of 32 IHA parameters adopted in this study

IHA Parameters Hydrological Parameters		
Group 1: Monthly Flow Magnitude	Mean or median discharge for each month (Includes 12 parameters)	
	- Annual minimum 1-day average flow	
	- Annual minimum 3-day average flow	
	- Annual minimum 7-day average flow	
	- Annual minimum 30-day average flow	
	- Annual minimum 90-day average flow	
Group 2: Magnitude and Duration	- Annual maximum 1-day average flow	
of Annual Extreme Flows	- Annual maximum 3-day average flow	
	- Annual maximum 7-day average flow	
	- Annual maximum 30-day average flow	
	- Annual maximum 90-day average flow	
	- Number of zero-flow days	
	- Base flow index: mean or minimum 7-day flow per year (12 parameters	
	total)	
Group 3: Timing of Annual - Date of minimum 1-day flow occurrence		
Extreme Flows	- Date of maximum 1-day flow occurrence	
	- Number of low flow pulses per year	
Group 4: Frequency and Duration of	- Number of high flow pulses per year	
High/Low Pulses	- Mean or median duration of low flow pulses (in days)	
	- Mean or median duration of high flow pulses (in days)	
	- Rise rate: mean or median of all positive differences between	
Group 5: Rate and Frequency of	consecutive daily flows	
Flow Changes	- Fall rate: mean or median of all negative differences between	
	consecutive daily flows	

Table 4. List of 34 environmental flow component (EFC) parameters adopted in this study

EFC Parameters	Environmental Flow Components
Low Flows	Monthly low flows: mean or median low flow for each month
Extreme Low Flows	 Frequency of extreme low flows annually or seasonally Mean or median duration of extreme low flows (days) Peak flow (minimum during event) Timing of event (date of peak low flow)
High Flow Pulses	 Frequency of high flow pulses annually or seasonally Mean or median duration of high flow pulses (days) Peak flow (maximum during event) Rise rate Fall rate
Small Floods	 Frequency of small floods annually or seasonally Mean or median duration of small floods (days) Peak flow (maximum during event) Timing of event (day of year) Rise rate Fall rate
Large Floods	 Frequency of large floods annually or seasonally Mean or median duration of large floods (days) Peak flow (maximum during event) Timing of event (day of year) Rise rate Fall rate

2.5 Model Setup and Input Data

The overall framework of this study is illustrated in Figure 2 and includes the following steps:

- (1) collection of input data for the SWAT model;
- (2) downloading and bias-correcting CMIP6 climate data;
- (3) calibration and validation of the SWAT

model;

(4) integration of Sixth Assessment Report scenarios with the calibrated SWAT model; (5) calculation of extreme flow indicators using IHA metrics; and (6) comparison of extreme flow variations between the future period (2030–2050) and the historical baseline (1990–2019).

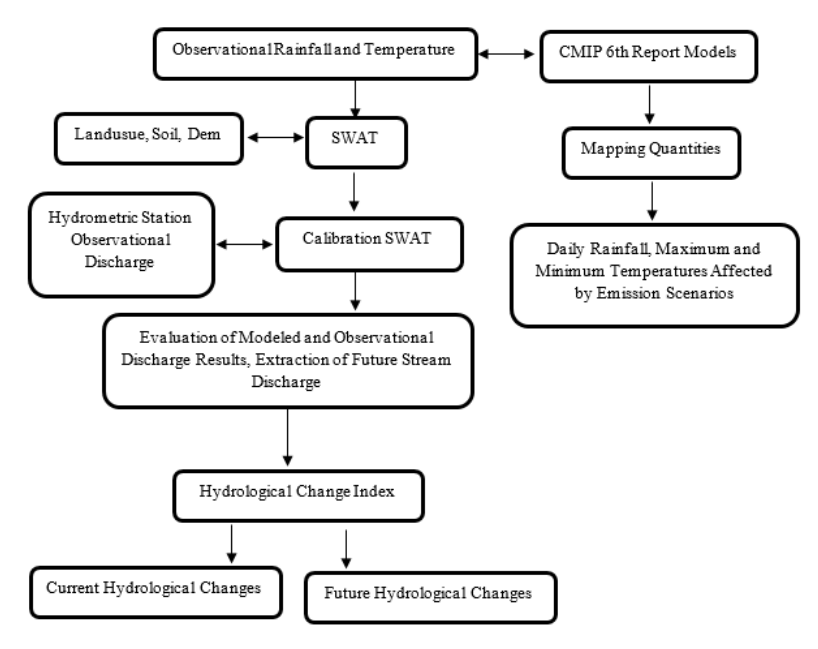


Figure 2. Flow chart of this study

The SWAT model requires three geophysical input layers: land use, soil type, and topography. The digital elevation data were derived from the Shuttle Radar Topography Mission (SRTM). Land use data (2015) were obtained from the Forest and Rangeland Organization, while soil data were extracted from the FAO-UNESCO soil map. Daily climate inputs to the SWAT model included precipitation, maximum, and minimum temperature, collected from regional meteorological stations for the period 1990-2019. Streamflow data from hydrometric stations were used for model calibration and validation.

Five slope classes (0–15%, 15–30%, 30–45%, 45–60%, and >60%) were defined during model setup. The next step involved delineating Hydrologic Response Units (HRUs), the most minor spatial units in SWAT, combining similar land-use, soil, and slope characteristics within each sub-basin for integrated hydrological computations.

SWAT has demonstrated reliable performance in simulating monthly streamflow under various climatic conditions in Kelantan, as well as historical drought events [Tan et al., 2010; Tan, 2017]. This study applied a new SWAT configuration calibrated using parameter

ranges and sensitivity analyses from previous studies [Tan et al., 2010; Tan, 2017]. The calibration and validation periods were set to 1994–2012 and 2013–2017, respectively, using observed flow data from the Pirdan hydrometric station on the Sarbaz River.

3. Results and Discussions

3.1. SWAT Calibration and Validation

The SWAT model was calibrated using the Sequential Uncertainty Fitting Version 2 (SUFI-2) algorithm within the SWAT-CUP software package. A total of 10,000 simulations were conducted during the calibration process to ensure convergence and robust parameter estimation. The following settings were used:

- Initial Parameter Ranges: Based on previous studies in similar climatic regions and sensitivity analysis results.
- Number of Iterations: 6 iterations were performed to refine parameter bounds and reduce uncertainty bands.
- Stopping Criterion: The calibration was stopped when the change in the objective function (P-factor and R-factor) between successive iterations fell below a predefined threshold (i.e., less than 1% improvement over two consecutive iterations).

- Sensitivity Analysis: Conducted before calibration to identify the most influential parameters, including ALPHA BF (baseflow recession coefficient), CN2 (SCS curve number), CH K2 (channel hydraulic conductivity).
- Performance Metrics: Nash–Sutcliffe Efficiency (NSE) and coefficient of determination (R²) were used as primary indicators of model performance.
- These settings ensured an effective balance between computational efficiency and model accuracy. The detailed configuration is summarized in Table 5 (below).

Table 5. The detailed configuration is summarized

Parameter	Initial	Final Calibrated
rarameter	Range	Value
ALPHA_BF	0.0 - 1.0	0.42
CN2	50 - 90	78

CH_K2	10-100 mm/hr	65 mm/hr
Number of Simulations	_	10,000
Number of Iterations	_	6
Stopping Criteria	_	<1% improvement over 2 iterations
Objective Functions	NSE, R ²	$NSE = 0.66, R^2 = 0.87$

Table 6 shows that the baseflow recession coefficient (ALPHA_BF), the SCS curve number for initial moisture conditions (CN2), and the effective hydraulic conductivity in the main channel alluvium (CH_K2) are the most sensitive parameters for calibrating monthly streamflow. ALPHA_BF reflects baseflow sensitivity to changes in groundwater recharge, while CN2 represents soil permeability, land use, and antecedent soil moisture conditions. At the same time, CH_K2 controls the exchange of water between groundwater and the river system.

Table 6. Final ranking of SWAT performance

Row	Parameter Name	Minimum Index	Maximum Index
1	v ALPHA BF.gw	0	1
2	v CH K2.rte	0	500
3	$\frac{-}{r}$ $\frac{-}{\text{CN2.mgt}}$	0.5-	0.5
4	v_ GW_DELAY.gw	0	500
5	r_SOL_AWC().sol	0.5-	0.5
6	vGW_REVAP.gw	0.02	0.2
7	vRCHRG_DP.gw	0	1
8	v_GWQMN.gw	0	5000
9	r_CH_N2.rte	0.5-	0.5
10	vREVAPMN.gw	0	500
11	vSURLAG.bsn	0.05	24
12	vESCO.bsn	0	1
13	v_CH_K2.rte	0	10
14	$r_{\overline{SOL}K(1).sol}$	-0.8	0.8
15	rSOL_BD(1).sol	-0.8	0.8
16	v_SFTMP.bsn	-20	20
17	vSMTMP.bsn	-20	20
18	v_SMFMX.bsn	0	20
19	v SMFMN.bsn	0	20
20	vTIMP.bsn	0	1
21	v_EPCO.bsn	0	1
22	vGWHT.gw	0	1
23	v_OV_N.hru	0	30

v_ indicates that the given value replaces the original parameter value. R means that the value of the parameter is added to the value of 1 and multiplied by the original value.

Figure 3 compares observed and simulated monthly streamflow at the Pirdan hydrometric station on the Sarbaz River during the calibration (1994–2012) and validation (2013–2018) periods. Overall, the simulated monthly flow shows a good agreement with the observed data. The model performance, evaluated using the coefficient of

determination (R^2) and Nash-Sutcliffe Efficiency (NSE), was ranked as "very good" for both the calibration period ($R^2 = 0.87$, NSE = 0.66) and validation period ($R^2 = 0.91$, NSE = 0.59), indicating reliable simulation capability at the monthly scale.

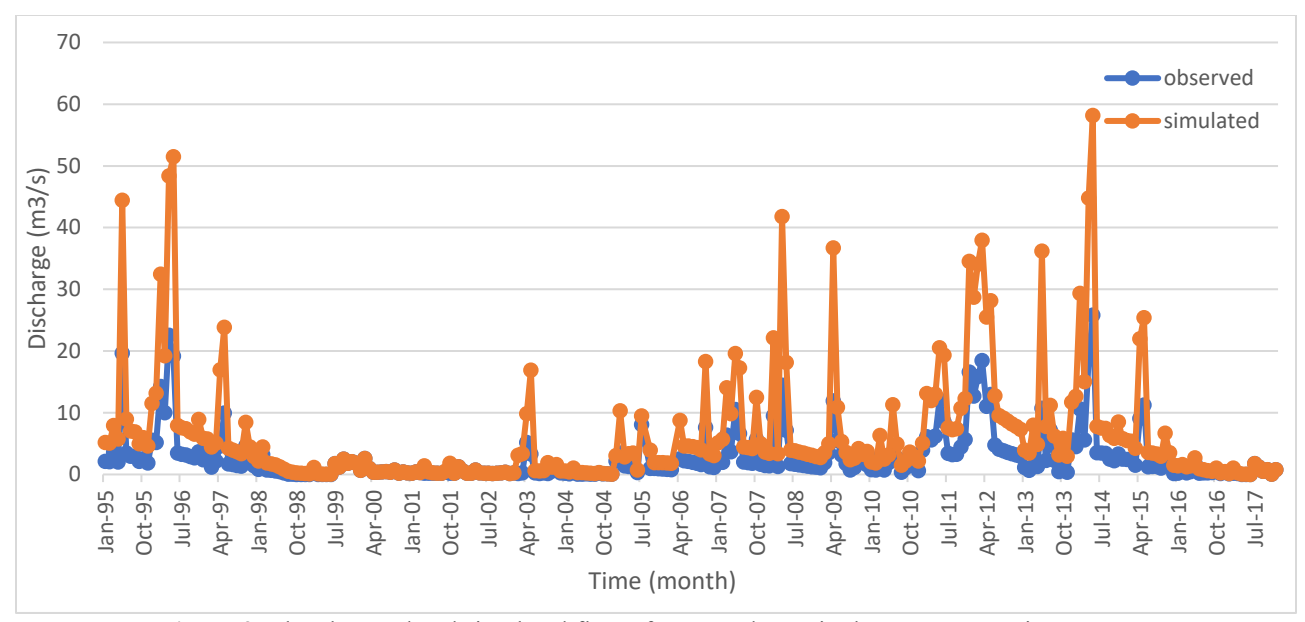


Figure 3. The observed and simulated flow of extracted swat in the swat cup environment

Figure 4 compares the climatology of monthly precipitation, maximum temperature, and minimum temperature from 1990 to 2014 based on observed data, raw CMIP6 models, and bias-corrected simulations. The raw CMIP6 models generally underestimate November and December precipitation, while an inconsistent pattern is observed in the other months. The HighResMIP models simulate the peak monthly rainfall one month earlier than observed, in November. The FGOALSf3-L model performs relatively poorly, significantly underestimating precipitation over KRB, particularly during the Southwest Monsoon (SWM) season (June to September).

Notably, the original HighResMIP models generally perform better at simulating

precipitation magnitude than the coarseresolution Regional Climate Models (RCMs) CORDEX-SEA, which from tend overestimate observed rainfall by up to 5 times in certain months in the same basin [Tan et al., 2020]. As shown in Figure 4d, the Quantile Mapping (QM) approach effectively corrects model biases in capturing the timing of monthly precipitation peaks (e.g., December) and the overall rainfall amounts simulations. Moreover, across all resolution (HR) simulations show less overestimation precipitation than lowresolution (LR) simulations during the study period.

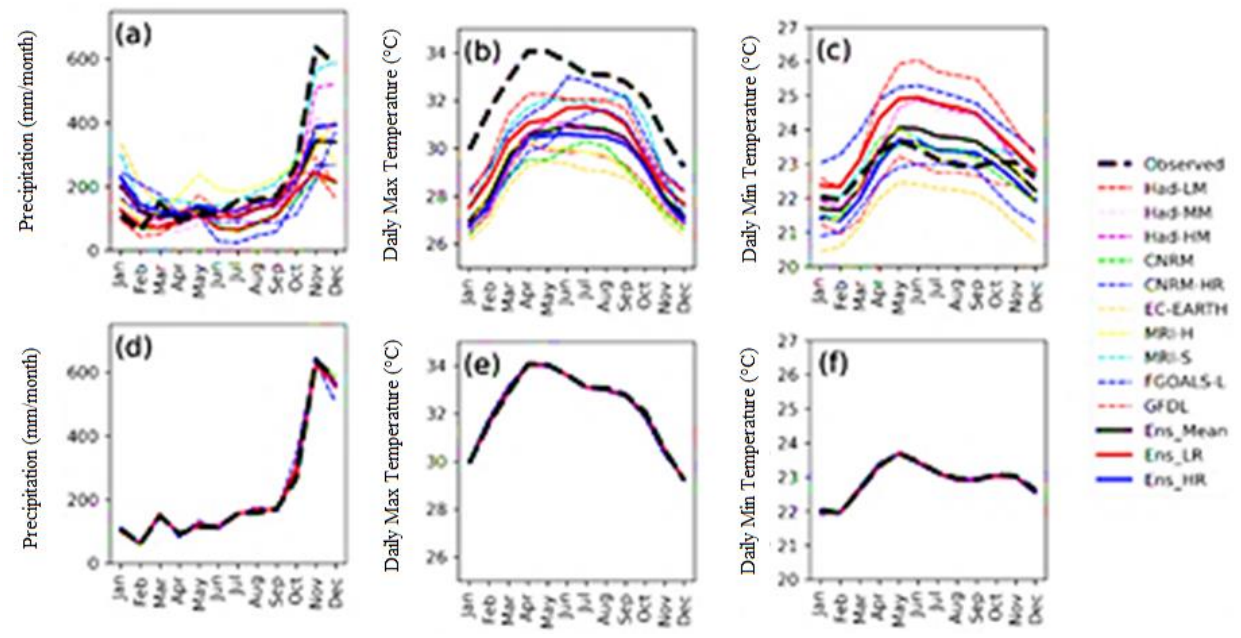


Figure 4. Annual cycles of monthly precipitation (a,d), monthly mean daily maximum (b,e), and minimum temperature (c,f) for the ten CMIP6 HighResMIP experiments, compared to observations during the period 1990~2014: a–c) original; (d–f) bias corrected for the Sarbaz River basin

Overall, most CMIP6 HighResMIP models reasonably capture the observed warm periods in April and September, as indicated by monthly averages of daily maximum and minimum temperatures (Figure 4b, c, e, f), particularly across inter-seasonal periods. However, all HighResMIP models tend to underestimate monthly maximum temperatures, while most of them overestimate monthly minimum temperatures, except for CNRM-CM6-1-HR, EC-EARTH3P, GFDL-CM4C192. Minimum temperatures in the climatological simulations performed better than maximum temperatures, as the ensemble mean was much closer to the observed data. Similar to precipitation, the biases in both maximum and minimum temperatures significantly reduced after applying Quantile Mapping (QM) bias correction method, as illustrated in Figures 4e and 4f. Compared to low-resolution (LR) simulations, high-resolution (HR) models show less overestimation of daily minimum However, significant temperatures. no improvement was found in the simulation of daily maximum temperatures in HR models.

3.2 Climate Change Projections

Figure 5 presents the projected annual and monthly changes in precipitation, daily maximum, and minimum temperatures over the period 2021–2050 relative to the historical baseline (1990–2014). Annual rainfall is projected to increase significantly by 6.9%. At the monthly scale, rainfall is expected to rise by 0.94% (October) to 15.1% (December), except in April, which shows a slight decrease of 2.4%. Statistically significant increases in monthly average precipitation are observed in June, July, August, and December (Figure 5a), indicating an overall upward trend in rainfall during these months.

The annual mean of daily maximum and minimum temperatures is projected to increase by 0.8 °C and 0.9 °C, respectively, during the future period compared to the historical period (Figure 5b). These warming trends are slightly higher than the long-term historical warming rates (0.1 °C/decade and 0.3 °C/decade for maximum and minimum temperatures, respectively) from 1990 to 2018. Every month, both maximum and minimum temperatures are expected to rise between 0.7–1.0 °C, with the

highest warming projected for May and November (Figure 5b).

Significant differences are evident between future and historical temperature averages at both annual and monthly scales (Figure 5b), supporting the existing literature on regional warming trends under a near-future climate scenario (the next 30 years).

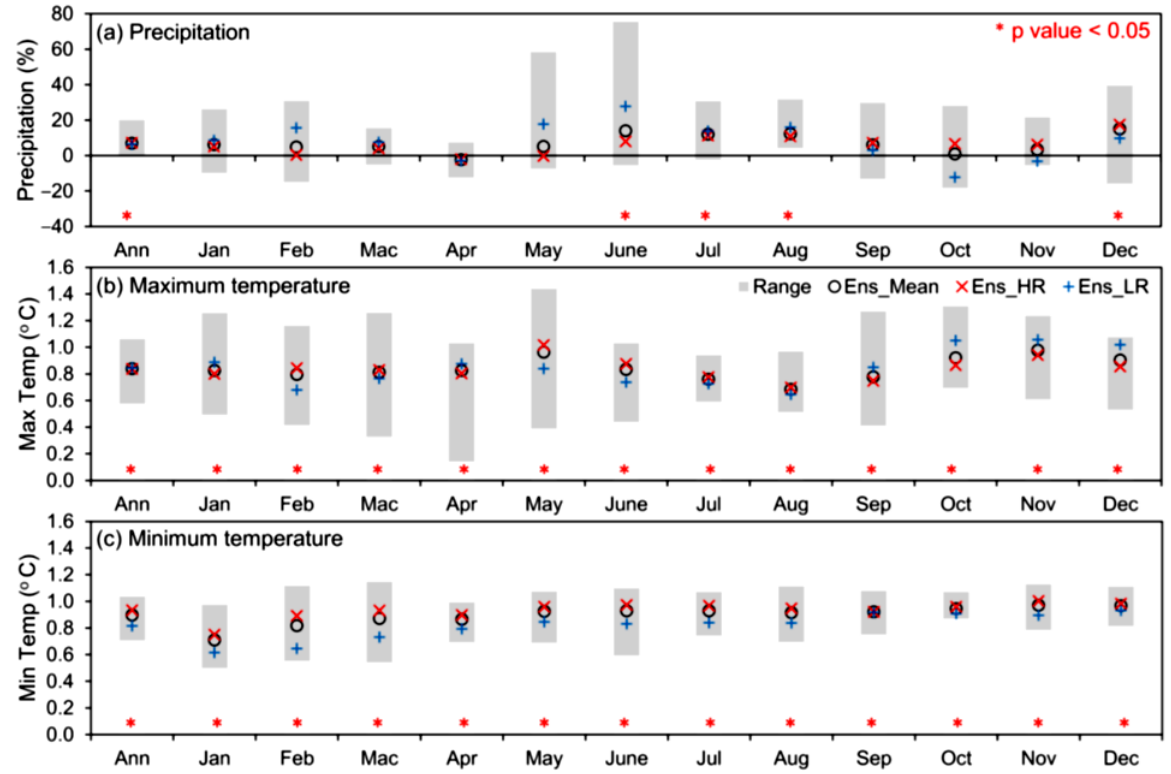


Figure 5. Projected changes in (a) precipitation, (b) maximum and (c) minimum temperatures between 2014 1990 and 2050 and 2021 in the Sarbaz river basin.

3.3 Hydrological Extremes Under Future Climate Conditions

Figure 6 compares projected hydrological extremes at the Pirdan hydrometric station on the Sarbaz River between the future period (2021–2050) and the historical baseline (1990– 2014). Annual and monthly streamflow are projected to increase by 9.9% and 3.5%-16.8%, respectively, based on the ensemble mean of 10 HighResMIP models. Higher increases (>10%) are expected during June to August and December. A statistically significant difference in mean flow at the 95% confidence level is observed at the annual scale and for specific months, including December-January, March, and June-October, mirroring the trends seen in projected monthly precipitation changes. In the next step, we analyze key indicators that define the magnitude of annual flow events over various durations, as outlined in the second group of Indicators of Hydrologic Alteration (IHA), listed in Table 1. As shown in Figure 6b,

the 1-, 3-, 7-, 30-, and 90-day minimum and maximum flows are projected to increase significantly between 7.2–8.2% and 10.4– 28.4%, respectively, during the future period. Notably, high variability is observed in extreme peak flows (1-, 3-, and 7-day maxima), suggesting a potential increase in flood magnitude in the near future. Regarding baseflow conditions, a slight decrease of 0.9% is projected for the future period. This suggests that groundwater contributions to streamflow may remain relatively stable compared to current levels, ensuring a similar freshwater supply capacity. However, if water demand rises due to future population growth, increased pressure on water resources could lead to potential water stress. The models project an increase in the magnitude of high-flow events, ranging from 1.0% to 25.3% (equivalent to 1.87 to 46.27 m³/s) for minimum flows and from 0.4% to 16.2% (0.73 to 29.67 m³/s) for maximum flows. This suggests that future

extreme flow events are likely to be delayed by several days to weeks compared to historical patterns. The fourth group of the Indicators of Hydrologic Alteration (IHA) captures the frequency and duration of extreme hydrological pulses. Results indicate no significant change in the number of low-flow pulses. However, a notable 22.7% increase in the number of high-flow pulses is projected. The duration of both low- and high-flow pulses is expected to change slightly, with ensemble mean changes of 3.3% and 5.9%, respectively.

The final IHA group evaluates the rate and frequency of flow condition transitions. A substantial increase of 31.9% in the rise rate and 25.5% in the fall rate is projected at the Pirdan station, indicating that rapid increases or decreases in streamflow are more likely in the future. Additionally, the number of hydrological reversals—daily flow shifts from increasing to decreasing, or vice versa—is projected to rise by 11.6%. This implies a greater frequency of abrupt flow fluctuations under future climate conditions.

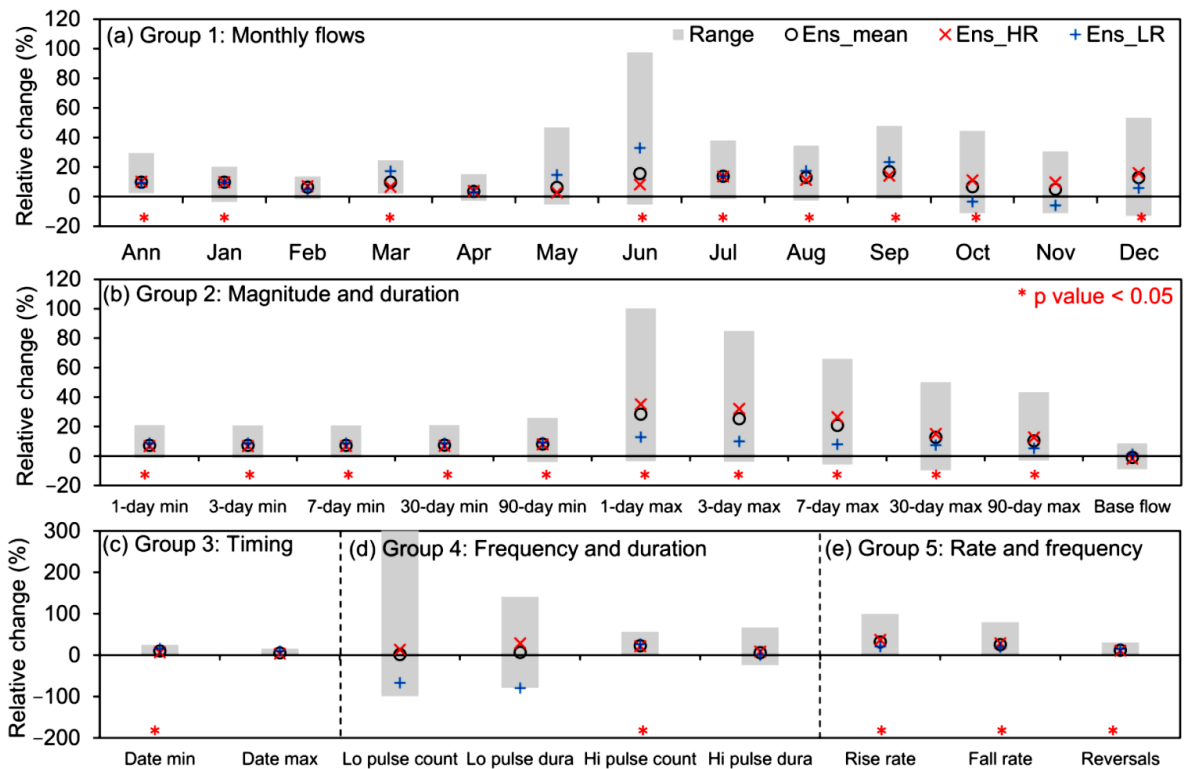


Figure 6. Projected changes in hydrological extremes represented by 32 IHA parameters of (a) monthly flows, (b) amount and duration, (c) timing, (d) frequency and duration, and (e) rate and frequency between the 1990s. -2014 is shown. and 2021–2050 at Pirdan station of Sarbaz river

3.4 Environmental Flow Condition (EFC) Changes

In this study, Environmental Flow Components (EFCs) were categorized into monthly low flows, extremely low flows, high-flow pulses, small floods, and large floods, given their critical importance in maintaining the ecological integrity of river systems. The first EFC group represents monthly groundwater-dependent low flows; therefore, any changes in these parameters may reflect shifts in groundwater availability. Overall, a slight

decrease in monthly low flows is projected for April, May, and October through December, ranging from 0.2% to 1.1%, based on ensemble-mean projections, as shown in Figure 7. In contrast, monthly low flows during July to September are expected increase to significantly by 4.3% to 9.4% at the 95% confidence level. The projected changes in EFCs could have significant ecological implications, including impacts on aquatic habitats, fish migration, and riparian vegetation. For instance, reductions in low flows during dry months may threaten the survival of species dependent on stable flow conditions, while increases in flood pulses could lead to habitat disturbance and erosion. Understanding these changes is crucial for developing sustainable water management plans that prioritize ecological flows and preserve riverine ecosystem health under future climate scenarios.

3.5. Discussion

Climate change is expected to exert a more significant influence on hydrological extremes compared to environmental flow components, as evidenced by a greater number substantial statistically **Indicators** Hydrologic Alteration (IHA) during the 2021-2050 period (Figure 6), in comparison to the Environmental Flow Components 7). Identifying indicators (Figure and understanding projected shifts in EFCs is vital for developing adaptive water management policies that balance ecological sustainability with human water demands. For instance, maintaining minimum flow levels during dry seasons is crucial for aquatic biodiversity, and alterations in flood pulse timing and magnitude may influence sediment transport and habitat connectivity. The statistical evaluation demonstrated that the SWAT model provided acceptable performance in simulating monthly streamflow. Changes in low flows and flood pulses directly influence the ecological health of riverine habitats. For example, reductions in groundwater-dependent low flows in certain months may degrade habitat for species that rely on stable flow conditions. At the same time, increases in high-flow pulses could erode spawning grounds and disrupt spawning. These shifts in EFCs are critical for understanding future hydrological resilience and conservation needs. One possible explanation for this reasonable performance could be the limited spatial density of rain gauges in the region, which may hinder the accurate representation of intense daily precipitation events at finer spatial resolutions [Bador et al., 2020]. Moreover, previous studies have indicated that the SWAT model tends to underestimate peak

flows in various regions, including river basins in Spain [Jimeno-Sáez et al., 2018], Brazil [Pereira et al., 2016], and Hawaii [Leta et al., 2016]. However, according to Crişan and Arnold [68], further research is required to evaluate whether model improvements can effectively address these limitations. Therefore, incorporating detailed analysis of these ecological flow components into future environmental and hydrological assessments is comprehensive essential for ecosystem management.

Climate projections are consistently regarded as one of the primary sources of uncertainty in hydroclimatic impact modeling [Kundzewicz et al., 2018]. Given that high-resolution (HR) models have been shown to better capture the characteristics of extreme precipitation events compared to their low-resolution (LR) counterparts [Liang et al., 2021], it can be expected that HR models provide more accurate assessments of future precipitation extremes. Among the models evaluated in this study, projected changes in future precipitation intensity differ significantly between HR and LR models. The average precipitation change during the January–December period is notably higher with HR models, with a peak increase of 9.6% compared to 5.0% with LR models (Figure 5). Similarly, the projected changes in monthly streamflow are significantly greater during the November–January period, reaching 11.8% for HR models compared to only 3.2% for LR models. Moreover, the magnitude and duration of maximum 1-day to 90-day flows show larger increases in HR models than in LR models, with the most significant differences observed in 1-day peak flows—projected to increase by up to 35.1% in HR models versus 12.8% in LR models (Figure 6). These results indicate that significant flood events under future climate scenarios are considerably more pronounced in HR model simulations than in LR models. For example, the frequency of large floods is projected to increase by 119% in HR models, compared to 44.4% in LR models (Figure 7).

This cross-comparison of simulations at different resolutions demonstrates that results from climate simulations with relatively coarse spatial resolution should be interpreted with caution. The relationship between model performance in simulating regional precipitation and its spatial resolution is complex. For instance, Liang et al. [2021] found that the high-resolution version of HadGEM3-GC3.1 showed a stronger ability to capture Borneo vortices during the Northeast Monsoon (NEM) season and their associated rainfall over Malaysia compared to its lowresolution counterpart. This partly explains why high-resolution simulations such as MRI-S and Had-HM reproduce the heavy rainfall periods (November and December) in the study area better than lower-resolution experiments, as shown in Figure 4a. We note that whether to use all available climate models or only those with superior performance in hydrological impact assessments remains a debated topic in optimal model selection [Kundzewicz et al., 2018].

Enhancing the quality of input data for hydrological simulations is crucial in climate impact studies [Tan et al., 2014; Wang et al., 2011], and is primarily based on statistical

approaches. For instance, Tan et al. [2017] applied a linear scaling method to correct biases in CMIP5 GCMs before using them as inputs in SWAT modeling. In this study, a statistical bias correction approach based on Quantile Mapping (QM) is employed to adjust biases in HighResMIP model experiments. This method has also been widely used for bias downscaled correction of dynamically simulations from CORDEX-SEA experiments over Malaysia [Ngai et al., 2020] and Southeast Asia [Ngai et al., 2017]. Shrestha et al. [2017] suggested that there may be no significant difference between simple (e.g., linear scaling) and more complex (e.g., QM) bias correction methods in monthly streamflow modeling. However, Luo et al. [2018] compared seven bias correction techniques using precipitation and temperature data from the Kaidu River basin in China and reported that the impact of the different correction schemes was more pronounced on rainfall than on temperature. Further research is needed to investigate how the choice of bias correction method affects GCM-based projections, and how Regional Climate Models (RCMs) influence daily streamflow simulations in the studied region and surrounding maritime continent areas.

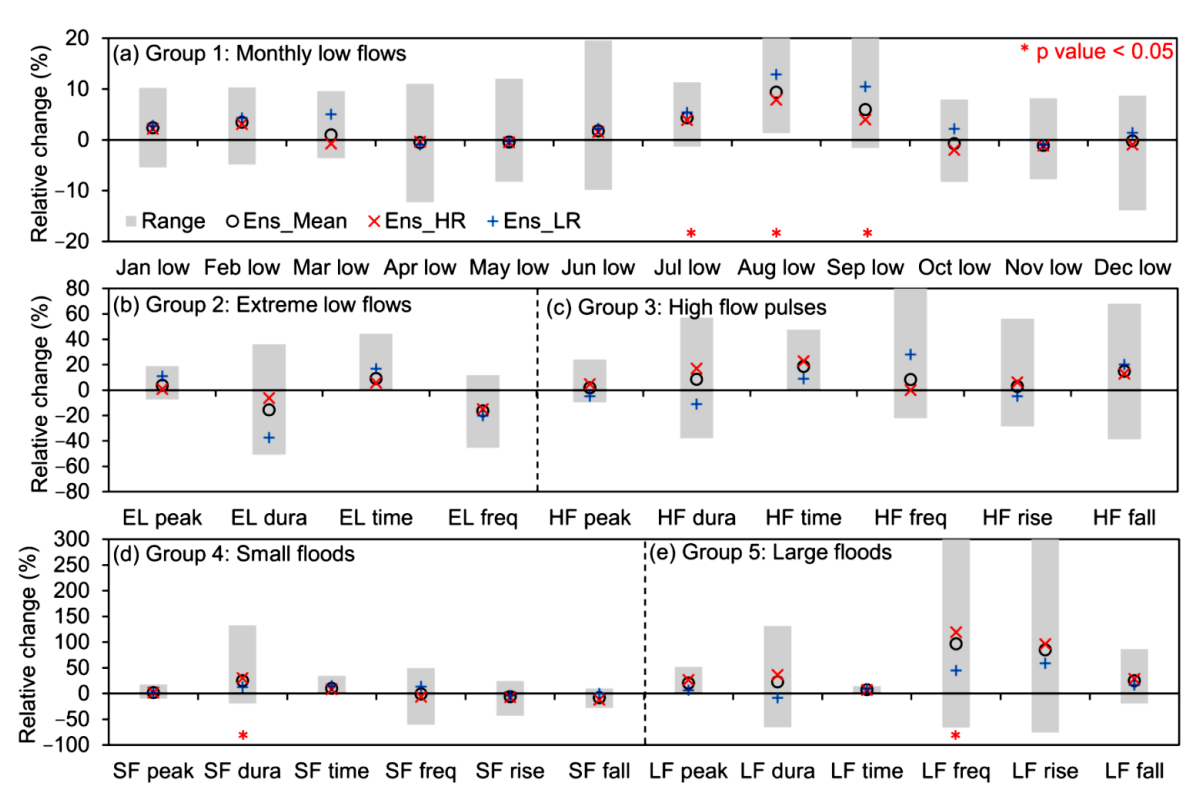


Figure 7. Projected changes in hydrological extremes represented by 32 EFC parameters (a) monthly low flow, (b) extreme low flow, (c) high flow pulses, (d) small floods and (e) large floods between Years 1990 to 2018 and 2021-2050 in Pirdan station of Sarbaz River

4. Conclusions

Extreme hydro-climatic events have significant impacts on both the environment and human society. This study integrates the latest high-resolution Global Climate Model (GCM) simulations from HighResMIP with the SWAT hydrological model to project potential future changes in hydrological extremes over the Kelantan River Basin (KRB). The SUFI-2 algorithm was applied for sensitivity analysis, calibration, and validation of the SWAT model, aiming to enhance its reliability in simulating long-term daily streamflow. During this process, ALPHA BF, CN2, and CH K2 identified as the most sensitive parameters in SWAT calibration, consistent with previous studies [Tan et al., 2020]. The raw outputs of HighResMIP experiments tend underestimate monthly precipitation during November and December. Additionally, the models simulate an earlier peak in monthly rainfall (approximately one month earlier) compared to observations. Most HighResMIP

experiments underestimate monthly maximum temperatures and overestimate minimum temperatures relative observations. Based on bias-corrected climate projections using the Quantile Mapping (QM) method, annual precipitation is projected to increase significantly by 6.9%. At the same time, maximum and minimum temperatures are expected to rise by 0.8 °C and 0.9 °C, respectively, during the 2021–2050 period compared to the baseline period (1990–2014). Monthly precipitation is projected to increase across nearly all months, ranging between 0.9% and 15.1%, except for March, which shows a slight decrease of 2.4%. Monthly maximum and minimum temperatures are also projected to rise by 0.7–1.0 °C.

Future simulations indicate a 9.9% increase in annual mean streamflow during the 2021–2050 period compared to the baseline period of 1990–2018. Concurrently, monthly streamflow is projected to rise by 3.5% to 16.8% across all months, with statistically significant changes observed. The magnitudes

of the 1-, 3-, 7-, 30-, and 90-day minimum and maximum flows are expected to increase notably, reaching up to 28.4%. In contrast, the baseflow index is projected to experience only minor changes, with a slight decrease of approximately 0.9%. The timing of extreme flow events is expected to shift, with delays of several days to weeks in their occurrence. The duration of both low- and high-flow pulses is anticipated to show only minor variations compared to the baseline period. However, the rise and fall rates of streamflow are projected to increase, indicating a higher likelihood of rapid increases or decreases in flow under future climate conditions.

For the 2021–2050 period, projections indicate a slight decrease in monthly low flows during April, May, October, November, and December compared to the baseline period of 1990-2018. In contrast, a significant increase in low flows ranging from 4.3% to 9.4% is expected from July to September. Future simulations also project reductions of 15.7% and 16.5% in the duration and frequency of extremely low flows. respectively. Regarding high-flow pulses, future projections show an increase of 1.8% to 18.6% compared to the baseline period. Overall, both small and large flood indices are projected to increase in the future. However, only the changes in the duration of minor floods and the frequency of large floods are statistically significant.

This study establishes a framework for the comprehensive assessment of hydro-climatic integrating extremes hydrological by high-resolution with climate modeling simulations. Further research is needed to better understand the SWAT model's limited ability to capture both peak and low flows. As more CMIP6 GCM simulations at varying model resolutions become publicly available, a comprehensive investigation into how horizontal and vertical resolutions of GCMs influence **SWAT** simulations will conducted in the near future. Ultimately, this study demonstrates that both high- and lowresolution climate models yield substantially different projections of future hydroclimatic extremes. Therefore, a quantitative climate forecasting framework combined with ensemble-based techniques should be developed to minimize uncertainties in extreme event simulations.

One notable limitation of this study is the mismatch in temporal resolution between the SWAT hydrological model calibration and the Indicators of Hydrologic Alteration (IHA) used to assess flow regime changes. The SWAT model was calibrated using monthly observed streamflow data, whereas several IHA indicators—particularly those related to extreme flows (e.g., 1-day, 3-day, and 7-day minimum and maximum flows)—require time-step data for accurate daily representation. This discrepancy may affect the precision of the IHA-based assessment, especially for short-term hydrological events. While monthly-scale calibration ensures reasonable accuracy in capturing long-term trends and seasonal variations, it may not fully capture the dynamics of short-duration highand low-flow events, which are critical for ecological and environmental flow assessments. Although daily simulated flow data were extracted from the model for IHA calculations, the lack of daily calibration limits the confidence in these results.

Therefore, future studies should aim to calibrate the SWAT model at a daily time step using high-resolution observed flow data to improve the reliability of IHA-based analyses. In the absence of such data, caution is advised when interpreting the ecological implications derived from IHA indicators in this study.

References

Abbaspour, K.C.; Vaghefi, S.A.; Srinivasan, R. A Guideline for Successful Calibration and Uncertainty Analysis for Soil and Water Assessment: A Review of Papers from the 2016 International SWAT Conference. Water 2018, 10, 18.

Abbaspour, K.C.; Vejdani, M.; Haghighat, S. SWAT-CUP calibration and uncertainty programs for SWAT. In Modsim

- International Congress on Modeling & Simulation Land Water & Environmental Management Integrated Systems for Sustainability; Modeling and Simulation Society of Australia and New Zealand: Wageningen, New Zealand, 2007; Volume 364, pp. 1596–1602
- Arnold, J.G.; Srinivasan, R.; Muttiah, R.S.; Williams, J.R. Large area hydrologic modeling and assessment part I: Model development. JAWRA J. Am. Water Resour. Assoc. 1998, 34, 73–89.
- Arnold, J.G.; Moriasi, D.N.; Gassman, P.W.; Abbaspour, K.C.; White, M.J.; Srinivasan, R.; Santhi, C.; Harmel, R.D.; Van Griensven, A.; Van Liew, M.W.; et al. SWAT: Model use, calibration, and validation. Trans. ASABE 2012, 55, 1491–1508.
- Bowden, J.H.; Otte, T.L.; Nolte, C.G.; Otte, M.J. Examining Interior Grid Nudging Techniques Using Two-Way Nesting in the WRF Model for Regional Climate Modeling. J. Clim. 2012, 25, 2805–2823.
- Borah, D. & Bera, M. 2004. Watershed-scale hydrologic and nonpoint-source pollution models: Review of applications. Transactions of the ASAE, 47, 789-803.
- Balti, H.; Ben Abbes, A.; Mellouli, N.; Farah, I.R.; Sang, Y.; Lamolle, M. A review of drought monitoring with big data: Issues, methods, challenges and research directions. Ecol. Inform. 2020, 60, 101136.
- Betts, R.A.; Alfieri, L.; Bradshaw, C.; Caesar, J.; Feyen, L.; Friedlingstein, P.; Gohar, L.; Koutroulis, A.; Lewis, K.; Morfopoulos, C.; et al. Changes in climate extremes, fresh water availability, and vulnerability to food insecurity are projected at 1.5 °C and 2 °C global warming with a higher-resolution global climate model. Philos. Trans. R. Soc. A Math. Phys. Eng. Sci. 2018, 376, 20160452.
- Daniel, E. B. 2011. Watershed Modeling and its Applications: A State-of-the-Art Review. The Open Hydrology Journal, 5, 26-50.

- Eyring, V.; Bony, S.; Meehl, G.A.; Senior, C.A.; Stevens, B.; Stouffer, R.J.; Taylor, K.E. Overview of the Coupled Model Intercomparison Project Phase 6 (CMIP6) experimental design and organization. Geosci. Model Dev. 2016, 9, 1937–1958.
- Fu, G., Barber, M. E. & Chen, S. 2010. Hydroclimatic variability and trends in Washington State for the last 50 years. Hydrological Processes, 24, 866-878.
- François, B.; Schlef, K.E.; Wi, S.; Brown, C.M. Design considerations for riverine floods in a changing climate—A review. J. Hydrol. 2019, 574, 557–573.
- Fu, B., Merritt, W. S., Croke, B. F. W., Weber, T. R. & Jakeman, A. J. 2019. A review of catchment-scale water quality and erosion models and a synthesis of prospects. Environmental Modeling & Software, 114, 75-97.
- Giorgi, F., Coppola, E. & Raffaele, F. 2018. Threatening levels of cumulative stress due to hydroclimatic extremes in the 21st century. npj Climate and Atmospheric Science, 1, 18.
- Gassman, P. W., Reyes, M. R., Green, C. H. & Arnold, J. G. 2007. The Soil and Water Assessment Tool: Historical Development, Applications, and Future Research Directions. Transactions of the ASABE, 50, 1211-1250.
- Gassman, P.W.; Reyes, M.R.; Green, C.H.; Arnold, J.G. The Soil and Water Assessment Tool: Historical Development, Applications, and Future Research Directions. Trans. ASABE 2007, 50, 1211–1250.
- Ghorbani Fard, M., 2021. Comparison and evaluation of AWBM and IHACRES models in rainfall-runoff modeling (Case study: catchment),10th International Conference on Rainwater Catchment System, ICRWC, 24-25 November 202021, University of Kurdistan, Iran. https://civilica.com/doc/1411242
- Haarsma, R.J.; Roberts, M.J.; Vidale, P.L.; Senior, C.A.; Bellucci, A.; Bao, Q.; Chang, P.; Corti, S.; Fu'ckar, N.S.; Guemas, V.; et

- al. High Resolution Model Intercomparison Project (HighResMIP v1.0) for CMIP6. Geosci. Model Dev. 2016, 9, 4185–4208.
- Harris, L.M.; Durran, D.R. An Idealized Comparison of One-Way and Two-Way Grid Nesting. Mon. Weather Rev. 2010, 138, 2174–2187
- Ipcc 2013. Climate Change 2013: The Physical Science Basis. Contribution of Working Group I to the Fifth Assessment Report of the Intergovernmental Panel on Climate Change Cambridge University Press, Cambridge, United Kingdom and New York, NY, USA,
- Kundzewicz, Z. W., Krysanova, V., Benestad, R. E., Hov, Ø., Piniewski, M. & Otto, I. M. 2018. Uncertainty in climate change impacts on water resources. Environmental Science & Policy, 79, 1-8.
- Kim, Y.-H.; Min, S.-K.; Zhang, X.; Sillmann, J.; Sandstad, M. Evaluation of the CMIP6 multi-model ensemble for climate extreme indices. Weather Clim. Extrem. 2020, 29, 100269
- Mohseni, B., Mahdavi, M. J., & Ghorbani fard, M. (2023). Assessing the Evaluation of Global and Regional Soil Maps in Flow Forecasting using SWAT Model (Talar Watershed, of Mazandaran Province). Geographical planning of space quarterly journal, 13 (2), 37-53. http://doi.org/10.30488/GPS.2023.379075. 3608
- Nash, J.E.; Sutcliffe, J.V. River flow forecasting through conceptual models part I—A discussion of principles. J. Hydrol. 1970, 10, 282–290
- Okwala, T.; Shrestha, S.; Ghimire, S.; Mohanasundaram, S.; Datta, A. Assessment of climate change impacts on water balance and hydrological extremes in Bang Pakong-Prachin Buri river basin, Thailand. Environ. Res. 2020, 186, 109544.
- Raghavan, S.V.; Tue, V.M.; Shie-Yui, L. Impact of climate change on future stream

- flow in the Dakbla river basin. J. Hydroinform. 2013, 16, 231–244.
- Raikes, J., Smith, T. F., Jacobson, C. & Baldwin, C. 2019. Pre-disaster planning and preparedness for floods and droughts: A systematic review. International Journal of Disaster Risk Reduction, 38, 101207.
- Shepherd, B., Harper, D. & Millington, A. 1999. Modelling catchment-scale nutrient transport to watercourses in the U.K. Hydrobiologia, 395-396, 227-238.
- Singh, V. & Woolhiser, D. 2002. Mathematical Modeling of Watershed Hydrology. Journal of Hydrologic Engineering, 7, 270-292
- Supari; Tangang, F.; Juneng, L.; Cruz, F.; Chung, J.X.; Ngai, S.T.; Salimun, E.; Mohd, M.S.F.; Santisirisomboon, J.; Singhruck, P.; et al. Multi-model projections of precipitation extremes in Southeast Asia based on CORDEX-Southeast Asia simulations. Environ. Res. 2020, 184, 109350.
- Tan, M.L.; Juneng, L.; Tangang, F.T.; Chung, J.X.; Radin Firdaus, R.B. Changes in Temperature Extremes and Their Relationship with ENSO in Malaysia from 1985 to 2018. Int. J. Climatol. 2021, 41, E2564–E2580. [CrossRef]
- Tong, S.; Li, X.; Zhang, J.; Bao, Y.; Bao, Y.; Na, L.; Si, A. Spatial and temporal variability in extreme temperature and precipitation events in Inner Mongolia (China) during 1960–2017. Sci. Total Environ. 2019, 649, 75–89. [CrossRef] [PubMed]
- Tan, M.L.; Gassman, P.; Yang, X.; Haywood, J. A Review of SWAT Applications, Performance and Future Needs for Simulation of Hydro-Climatic Extremes. Adv. Water Resour. 2020, 143, 103662.
- Tan, M. L., Ficklin, D., Ibrahim, A. L. & Yusop, Z. 2014. Impacts and uncertainties of climate change on streamflow of the Johor River Basin, Malaysia using a CMIP5 General Circulation Model ensemble. Journal of Water and Climate Change, 5, 676–695

- Vannière, B.; Demory, M.-E.; Vidale, P.L.; Schiemann, R.; Roberts, M.J.; Roberts, C.D.; Matsueda, M.; Terray, L.; Koenigk, T.; Senan, R. Multi-model evaluation of the sensitivity of the global energy budget and hydrological cycle to resolution. Clim. Dyn. 2019, 52, 6817–6846.
- Zhang, H.; Wang, B.; Liu, D.L.; Zhang, M.; Leslie, L.M.; Yu, Q. Using an improved SWAT model to simulate hydrological responses to land use change: A case study of a catchment in tropical Australia. J. Hydrol. 2020, 585, 124822.